International Immunopharmacology 71 (2019) 336–349

Contents lists available at ScienceDirect

International Immunopharmacology

journal homepage: www.elsevier.com/locate/intimp

UCP2 ameliorates mitochondrial dysfunction, inflammation, and oxidative stress in lipopolysaccharide-induced acute kidney injury

Yue Ding[a,1], Yijun Zheng[a,1], Jinda Huang[a], Wanwan Peng[a], Xinxin Chen[a], Xiangjin Kang[b,*], Qiyi Zeng[a,*]

[a] Department of Pediatrics, Zhujiang Hospital, Southern Medical University, 253 Gongye Road, Guangzhou 510280, Guangdong, China
[b] Center for Reproductive Medicine, Third Affiliated Hospital of Guangzhou Medical University; Key Laboratory for Reproductive Medicine of Guangdong Province; Key Laboratory for Major Obstetric Diseases of Guangdong Province; Key Laboratory of Reproduction and Genetics of Guangdong Higher Education Institutes, Guangzhou 510150, Guangdong, China.

ARTICLE INFO

Keywords:
LPS
Acute kidney injury
Uncoupling protein 2
Mitochondrial
Inflammation
Oxidative stress

ABSTRACT

Objective: UCP2 is involved in the maintenance of mitochondrial function, immune response and regulation of oxidative stress under physiological or pathological conditions. The aim of this study was to investigate the effects of UCP2 on mitochondrial dysfunction, inflammation, and oxidative stress in septic acute kidney injury (AKI).

Methods: We established LPS-induced AKI model in mice and HK-2 cells. In vivo, the UCP2 inhibitor genipin was used to downregulate UCP2 in mouse kidneys. In vitro, UCP2 overexpression or knockdown was achieved by LV5-UCP2 or si-UCP2 transfection, respectively, to characterize the mechanisms of UCP2 in septic AKI. Indicators of renal injury, cell apoptosis, inflammation, oxidative stress, and mitochondrial dysfunction were assessed.

Results: Compared to the control group, LPS treatment increased UCP2 expression in vitro and in vivo. In vitro, UCP2 overexpression protected HK-2 cells from LPS-induced injury by suppression of apoptosis, inflammation, oxidative stress, MMP loss and ROS production, increase of ATP production and mtDNA content, and amelioration of damage to the mitochondrial ultrastructure. Additionally, inhibition of UCP2 expression by si-UCP2 resulted in decreased HK-2 cell resistance to LPS toxicity, as shown by increased apoptosis, inflammation, mitochondrial dysfunction and oxidative stress. In vivo, UCP2 downregulation aggravated the LPS-induced renal injury, inflammation, macrophages infiltration, mitochondrial dysfunction, and oxidative stress.

Conclusion: UCP2 may protect LPS-induced AKI by ameliorating mitochondrial dysfunction, anti-inflammation, and antioxidative activities, ultimately inhibiting tubule epithelial cell apoptosis, and that increasing the UCP2 content in mitochondria constitutes a new therapeutic approach for septic AKI.

1. Introduction

Sepsis is a life-threatening organ dysfunction caused by a dysregulated host response to infection [1]. It is estimated to affect at least 1–1.5 million persons each year in the USA [2–5], and 19 million patients worldwide [6,7]. Despite advances in critical care, sepsis remains a highly lethal entity resulting in > 200,000 USA deaths per year and an in-hospital mortality upward of 30% [4,5]. In critically ill patients, AKI is a common and serious complication of sepsis, and sepsis is the leading cause of AKI in the intensive care unit (ICU), accounting for 45–70% of all AKI [8]. In the recent Vasopressin vs. Norepinephrine as Initial Therapy in Septic Shock (VANISH) trial, AKI occurred in about 45% of patients, and AKI requiring renal replacement therapy (RRT) developed in 30% of patients [9]. The development of septic AKI is associated with increased mortality, and survivors are at risk of developing chronic kidney disease, which is a burden for both patients and society [10]. Septic AKI is a multifactorial syndrome, and the current understanding of its pathogenesis involves microcirculatory abnormalities, mitochondrial dysfunction and inflammatory changes [11,12].

Mitochondria have important roles in both physiological and pathophysiological processes, including calcium homeostasis, cell signaling pathways, transcriptional regulation, and apoptosis [13]. The heart and kidney possess the greatest abundances of mitochondria,

* Corresponding authors.
E-mail addresses: kangxiangjin@163.com (X. Kang), zqy_88@163.com (Q. Zeng).
[1] These authors contribute equally to this work.

https://doi.org/10.1016/j.intimp.2019.03.043
Received 5 March 2019; Accepted 21 March 2019
Available online 02 April 2019

which work cooperatively to provide energy [14]. Multiple aspects of mitochondrial dysfunction, such as the overproduction of reactive oxygen species (ROS), the depletion of adenosine triphosphate (ATP), the disruption of mitochondrial membrane potential (MMP or ΔΨm), and the exacerbation of apoptosis, are thought to influence septic AKI [13]. Moreover, previous studies have suggested that the intersection between mitochondrial biogenesis and the inflammatory response is important in disease [15]. In septic AKI, inflammation at the tissue and cellular levels is associated with mitochondrial injury and with decreased levels of intracellular ATP in the kidney [16]. Therefore, evolving strategies for targeting mitochondrial dysfunction hold promise for the prevention and treatment of septic AKI.

Uncoupling proteins (UCPs), members of the anionic proton transporter family, which are located in the mitochondrial inner membrane, can promote proton leakage across the inner membrane. They are the essential regulator of MMP and disperses the mitochondrial proton gradient by translocating H+ across the inner membrane, with subsequent respiratory activity and ROS and ATP generation [17]. Uncoupling protein 2 (UCP2) is the most well-known protein in its family, as it is ubiquitously expressed in multiple tissue types, such as those of the central nerve system, kidney, heart, liver, pancreas, spleen, thymus and macrophages [18]. The wide distribution of UCP2 leads to its regulation of numerous metabolic processes, such as ATP and ROS production; mitochondrial calcium balance and MMP stabilization; and glucose control, in addition to regulation of immunity and multiple pathologies, such as sepsis, diabetes, and cancer [19]. However, the pathological function of UCP2 was found to be tissue- and disease-specific. UCP2 overexpression reverses sepsis-induced myocardial injuries by reducing ROS production and regulating mitoflash frequency [20]. UCP2 plays a cytoprotective role in the lung and spleen via its antioxidant synergy with mt-iPLA2γ [21]. In contrast, some studies have shown that UCP2 increases susceptibility to LPS-induced acute lung and liver injury in mice [22,23]. UCP2 deficiency provides protection in a murine model of endotoxemic acute liver failure [24].

In early experiments, we found that UCP2 expression was increased in septic kidney tissue [25]. However, the functional role of UCP2 in septic AKI remains to be determined. We hypothesized that UCP2 regulated mitochondrial function, inflammation and oxidative stress in septic AKI. In the present study, we explored the association between mitochondrial dysfunction and UCP2 expression. Our findings indicated that UCP2 ameliorated mitochondrial dysfunction, inflammation, and oxidative stress in lipopolysaccharide-induced AKI, suggesting that UCP2 may be a novel treatment target for LPS-induced AKI.

2. Materials and methods

2.1. Cell culture, transfection and septic AKI cell model

A human proximal tubule epithelial cell line (China Center for Type Culture Collection, Wuhan, China), HK-2 cells, was cultured in Minimum Essential Medium (MEM; Gibco, Carlsbad, CA, USA) containing 10% fetal bovine serum (FBS), 1% nonessential amino acids (NEAA) and antibiotics (100 U/ml penicillin G, 100 μg/ml streptomycin) at 37 °C in a cell culture incubator with 5% CO_2 and saturation humidity. For overexpression of UCP2, when the HK-2 cells were 50% confluent in fresh serum-free medium, they were transiently transfected with UCP2-overexpression lentivirus (LV5-UCP2) or negative control lentivirus (LV5-NC) at a multiplicity of infection (MOI) of 20. The cells were cultured in MEM with 10% FBS and 1% NEAA after infection for 4 h and then selected using 2 μg/ml puromycin. Stable overexpression lines were established when > 90% of the transfected cells were found to strongly express GFP under a fluorescence microscope. For inhibition of UCP2 expression, cells were cultured in six-well tissue culture plates for 24 h until they reached 30–50% confluence. Then, small interfering RNAs targeting UCP2 (si-UCP2) or a negative control (si-NC), synthesized by Shanghai GenePharma Co., Ltd. (Shanghai, China), were transfected into cells using RNAiMAX (Invitrogen Life Technologies, Carlsbad, CA, USA) according to the manufacturer's instructions.

To construct a septic AKI cell model, nontransfected or transfected HK-2 cells were exposed to LPS (*Escherichia coli* 0111:B4; Sigma, St. Louis, MO, USA; 100 μg/ml) [26]. Cells were divided into the following six groups: control, LPS, LV5-NC-transfected + LPS (LV5-NC + LPS), si-NC-transfected + LPS (si-NC + LPS), LV5-UCP2-transfected + LPS (LV5-UCP2 + LPS), and si-UCP2-transfected + LPS (si-UCP2 + LPS).

2.2. Septic AKI mouse model

Male C57BL/6J mice weighing 18–22 g ($n = 24$) were obtained from the Experimental Animal Center at Southern Medical University (GuangZhou, China). All experimental procedures were performed in strict accordance with the PR China Legislation Regarding the Use and Care of Laboratory Animals, and all experiments were approved by the Animal Care and Use Committee of Southern Medical University.

Mice were divided into the following groups containing 8 mice per group: control, LPS-treated (LPS) and Genipin + LPS-treated (Genipin + LPS). To establish the septic AKI model, mice were intraperitoneally injected with LPS at a dose of 15 mg/kg body weight [23]. Genipin (Dalian Meilunbio Co., Ltd., DaLian, China) was injected by gavage 1 h before LPS administration at a dose of 100 mg/kg body weight [27]. Saline was used as the negative control. On the basis of the results of a preliminary experiment, animals were sacrificed 24 h after LPS injection. Blood samples were obtained from the mice and centrifuged to produce serum. Then, the blood and the kidney samples were stored at −80 °C for further analysis.

2.3. Assessments of biochemical parameters of renal function in serum

The serum BUN and Cr levels were measured using commercial kits (Nanjing Jiancheng Bioengineer Institute, Nanjing, China). Neutrophil gelatinase-associated lipocalin (NGAL) and kidney injury molecule 1 (KIM-1) were measured with an NGAL and a KIM-1 enzyme-linked immunosorbent assay (ELISA) kit, respectively (Cusabio Life Science, WuHan, China). Experimental procedures in the provided instruction manuals were strictly followed.

2.4. Histological and immunohistochemical assays

The kidney tissues were fixed in 10% formalin, embedded in paraffin, and sectioned into 5-μm sections. The sections were stained with hematoxylin-eosin (H&E). For the immunofluorescence staining of UCP2, NF-κB p65 and Galectin-3, tissue sections were incubated for 1 h with 3% hydrogen peroxide (H_2O_2) to block endogenous peroxidase and then incubated with 5% normal goat serum for 30 min. Next, the sections were incubated at 4 °C overnight with antibodies against UCP2, NF-κB p65 and Galectin-3 (Cell Signaling Technology, Inc., MA, USA; all dilutions were 1:50). After washing, a horseradish peroxidase (HRP)-labeled polymer antibody (Santa Cruz Biotechnology, CA, USA) was used as the secondary antibody. Diaminobenzidine (DAB) was used as the substrate, and sections were counterstained with hematoxylin. All sections were photographed using a light microscope (Nikon Eclipse TE2000-U, NIKON, Japan) at 400× magnification.

2.5. Cell viability and apoptosis assays

Cell viability was assessed with the Cell Counting Kit-8 (CCK-8, Dojindo Molecular Technologies, Kumamoto, Japan). HK-2 cells were seeded into 96-well plates at a density of 5×10^3 cells/well and treated with various concentrations of LPS (0, 1, 5, 10, 50 and 100 μg/ml) for 24 h. After LPS stimulation, 10 μl CCK-8 was added into each well and incubated for 4 h at 37 °C. The absorbance was measured at 450 nm using a microplate reader (Bio-Rad, Hercules, CA). On the basis of the CCK8 results, treatment with 100 μg/ml LPS for 24 h was selected for

subsequent experiments.

Quantitation of apoptotic cells was performed using an Annexin V-FITC/PI apoptosis detection kit and Annexin V-633/PI apoptosis detection kit (Dojindo Molecular Technologies, Kumamoto, Japan). Briefly, HK-2 cells or the transfected cells were seeded into 6-well plates at a density of 5×10^5 cells/well and subjected to 100 μg/ml LPS for 24 h. After washing in ice-cold phosphate-buffered saline (PBS) twice, cells were resuspended in 500 μl Binding Buffer containing 5 μl Annexin V-FITC or Annexinn V-633 and 5 μl PI. The samples were then incubated in the dark at room temperature for 15 min, and the apoptotic cells (Annexin V-FITC-positive or Annexinn V-633-positive and PI-negative) were distinguished on a flow cytometer (BD Biosciences, San Jose, CA, USA).

2.6. Quantitative real-time PCR analysis

Total RNA was extracted from the cells and kidney tissues using TRIZOL reagent (TaKaRa Biotechnology Co., Ltd., China) according to the manufacturer's protocol. Then, reverse transcription polymerase chain reaction (RT-PCR) was performed using the Prime-Script RT reagent kit (TaKaRa Biotechnology Co., Ltd., China) on a TC-512 PCR system (TECHNE, UK) after the concentration of the extracted RNA was measured. qPCR was performed using SYBR®Premix Ex Taq™II (Tli RNaseH Plus) (TaKaRa Biotechnology Co., Ltd., China). The threshold cycle (Ct) was obtained from triplicate samples and averaged. Calculations were based on the ΔΔCt method using the equation R (ratio) = $2^{-\Delta\Delta}$Ct and normalized to GAPDH expression in each sample. All primers were designed and synthetized by Sangon Biotech Co., Ltd. (Shanghai, China). The primer sequences are listed in Table 1.

2.7. Western blot analysis

The total protein samples from the cells and kidney tissues were homogenized using RIPA lysis buffer containing protease inhibitors and phosphatase inhibitor cocktail 2. The protein concentrations of the samples were determined using a BCA Protein Assay kit (Bio-Rad, Hercules, CA, USA) and standards. The proteins (50 μg) were denatured with sodium dodecyl sulfate (SDS) sample buffer, separated on 10% SDS-polyacrylamide gel electrophoresis (PAGE) gels, and transferred to PVDF membranes (Millipore, MA, USA). After being blocked with 5% BSA for 2 h at room temperature, the membranes were incubated with primary antibodies overnight at 4 °C. Antibodies against β-actin (42 kDa), UCP2 (32 kDa), p65 (65 kDa), pp65 (65 kDa), IκBα (39 kDa), p-IκBα (40 kDa) were supplied by Cell Signaling Technology. After the addition of the anti-rabbit secondary antibody for 1 h at room temperature, the protein signal was developed using ECL substrate (Beyotime Institute of Biotechnology, Jiangsu, China) according to the manufacturer's instructions. The immunoreactive protein bands were visualized using the In-Vivo Imaging System F (Eastman Kodak Co., Rochester, NY, USA). The band intensity was quantified using ImageJ software.

2.8. Enzyme-linked immunosorbent assay (ELISA)

Six hours after LPS treatment, the culture supernatants of HK-2 cells were collected for subsequent measurements of IL-6, IL-1β and TNF-α expression levels. The culture supernatants were measured using commercially available ELISA kits (Cusabio Life Science, Wuhan, China). All procedures were performed in strict accordance with the manufacturer's instructions. The samples were analyzed in triplicate.

2.9. MMP (or ΔΨm)

ΔΨm was assessed using a laser scanning confocal microscope (LSCM, FV10i-W; Olympus Corp., Tokyo, Japan) and a flow cytometer (BD FACSAria; BD Biosciences, Franklin Lakes, NJ, USA) with 5,5′,6,6′-tetrachloro-1,1′,3,3′-tetraethylbenzimidazole-carbocyanide iodine (JC-1; Beyotime Institute of Biotechnology) staining. The HK-2 cells and mitochondria isolated from kidneys were stained with JC-1 for 20 min at 37 °C after 24 h of incubation with LPS. Cells and mitochondria isolated from kidneys were examined using the LSCM, and cells were also evaluated by FCM. Fluorescence was read at 488 nm excitation and 530 nm emission for green and at 540 nm excitation and 590 nm emission for red. The ratio of aggregated JC-1 (red fluorescence) and monomeric JC-1 (green fluorescence) represented the ΔΨm.

2.10. Transmission electron microscopy (TEM) and analysis of mitochondrial damage

The cells treated per the group designation were washed with PBS and collected. After fixation in 2% glutaraldehyde, cells were dehydrated with an ascending acetone series, suspended in an acetone-Epon mixture, embedded in Epon using capsules (Piano, Marburg, Germany) and polymerized. Each sample was cut and dyed with uranyl acetate and lead citrate and viewed under a transmission electron microscope (H-7650; Hitachi, Tokyo, Japan). To examine mitochondrial ultrastructure in vivo, fresh kidneys from different groups were cut into 1 mm^3 blocks, and subsequent steps were performed as described above for cells.

2.11. Measurement of intracellular ROS accumulation

The production of intracellular ROS in HK-2 cells was fluorometrically monitored using dihydroethidium (DHE) (Beyotime Institute of Biotechnology). Cells in 6-well culture dishes were trypsinized and collected by centrifugation. DHE, diluted to a final concentration of

Table 1
Primers sequences.

Genes	Species	Forward	Reverse
UCP2	Human	GGCTGGAGGTGGTCGGAGATAC	CAGCACAGTTGACAATGGCATTACG
GAPDH	Human	GCACCGTCAAGGCTGAGAAC	TGGTGAAGACGCCAGTGGA
TNF-α	Human	CGCGTTCATGTCGTAATAGTT	CGGGCCGATTGATCTCAGC
IL-1β	Human	AACCTCTTCGAGGCACAAGG	GGCGAGCTCAGGTACTTCTG
IL-6	Human	GGTACATCCTCGACGGCATCT	GTGCCTCTTTGCTGCTTTCAC
ND1	Human	CATTCCTAATGCTTACCGAACG	GTAGAGGGTGATGGTAGATGTG
LPL	Human	AAGAGAGAACCAGACTCCAATG	TATTGGTCAGACTTCCTGCAAT
UCP2	Mouse	CTCTACGACTCTGTCAAACAGT	GGACCTTTACCACATCTGTAGG
GAPDH	Mouse	ACCCCAGCAAGGACACTGAGCAAG	GGCCCCTCCTGTTATTATGGGGGT
TNF-α	Mouse	CCCAGACCCTCACACTCCAGAT	TTGTCCCTTGAAGAGAACCTG
IL-1β	Mouse	CACCTTCTTTTCCTTCATCTTTG	GTCGTTGCTTGTCTCTCCTTGTA
IL-6	Mouse	CTCCCAACAGACCTGTCTATAC	CCATTGCACAACTCTTTTCTCA
ND1	Mouse	CTAATCGCCATAGCCTTCCTAA	GTTGTTAAAGGGCGTATTGGTT
LPL	Mouse	CCTGATGACGCTGATTTTGTAG	CAATGAAGAGATGAATGGAGCG

10 μM with MEM, was added to the HK-2 cells followed by incubation at 37 °C for 20 min. Following treatment with DHE, HK-2 cells were washed 3 times with PBS. Intracellular ROS were quantified by FCM with 535 nm excitation and 590 nm emission. Data analysis was performed with CellQuest software and the mean fluorescence intensity was used to quantify the responses. A minimum of 10,000 cells were acquired for each sample.

2.12. Measurement of mtDNA content

The mtDNA content was measured by RT-PCR method. Total intracellular DNA was isolated by using a QIAamp DNA Mini Kit (Qiagen, Hilden, Germany). RT-PCR reactions were carried out in a total volume of 10 μl according to the manufacturer's protocol. NADH dehydrogenase subunit 1 (ND1) was on behalf of mtDNA amplification and lipoprotein lipase (LPL) was on behalf of an internal control. Compared the relative amount of mtDNA with nuclear DNA (nDNA) copy numbers, the ddCT (ND1/LPL) represented the mtDNA copy number in a cell. All primers were designed and synthetized by Sangon Biotech Co., Ltd. (Shanghai, China). The primer sequences are also listed in Table 1.

2.13. Biochemical analyses

Methods for the total protein extraction from kidney tissues and HK-2 cells are the same as those mentioned before. ATP level was measured using a firefly luciferase-based ATP assay kit (Beyotime Institute of Biotechnology). Chemicals used for measuring superoxide dismutase (SOD) activity and malondialdehyde (MDA) levels were obtained from Nanjing Jiancheng Bioengineering Institute (Nanjing, China).

2.14. Statistical analysis

The experimental values were obtained from 3 independent experiments with a similar pattern and are expressed as the means ± SD. For the determination of the significant differences between the control and treatment groups, we used ANOVA, followed by post hoc pairwise comparison (LSD) tests for analysis. Statistical analysis was carried out using the SPSS software package 20.0. Statistical significance was set at $p < .05$.

3. Results

3.1. Up- or downregulation of UCP2 expression by UCP2 recombinant lentiviral (LV5-UCP2) or si-UCP2 transfection in HK-2 cells

To determine the role of UCP2 in LPS-induced AKI, the expression of UCP2 was up- or downregulated by LV5-UCP2 or si-UCP2 transfection, respectively, and cells transfected with LV5-NC or si-NC served as control groups. The mRNA level of UCP2 was increased by 3.74-fold following transfection with LV5-UCP2 compared with transfection with LV5-NC, which was consistent with an increase in UCP2 protein expression (Fig. 1A and B). The mRNA level of UCP2 was reduced by approximately 45.65% following transfection with si-UCP2 compared with transection with si-NC, which was consistent with a decrease in UCP2 protein expression (Fig. 1A and B). No significant changes in UCP2 mRNA and protein levels were observed in the cells transfected with LV5-NC or si-NC compared with the control group.

3.2. UCP2 expression in LPS-induced AKI

Fig. 2A, B and C shows that after LPS exposure, the UCP2 mRNA and protein expression levels were markedly increased compared with control group in mouse kidneys. Next, a pharmacological inhibitor of UCP2, genipin, was used to downregulate the expression of UCP2. Pretreatment with genipin resulted in a significant blockade of the LPS-induced upregulation of the UCP2 mRNA and protein expression levels. As shown in Fig. 2D, both the UCP2 mRNA and protein expression levels in HK-2 cells were increased in a time-dependent manner after LPS exposure.

3.3. UCP2 inhibition by genipin pretreatment promotes LPS-induced renal injury

The serum BUN, Cr, KIM-1 and NGAL levels are considered important biochemical markers of the severity of renal injury. As shown in Fig. 3A, the serum BUN, Cr, KIM-1 and NGAL levels were remarkably elevated in the LPS-treated mice compared with control mice. Subsequently, we explored the effects of genipin on renal injury under septic conditions. Pretreatment with genipin in LPS-treated mice further increased the serum BUN, Cr, KIM-1 and NGAL levels.

Intraperitoneal injection of LPS also resulted in serious pathological damage to the kidney. As observed with H&E staining, we found that LPS caused tissue damage mainly in the renal cortex and outer medulla. As shown in Fig. 3B, compared with control group, the histopathological changes in the kidneys of LPS group included partial renal tubular epithelial vacuole degeneration, or hyaline degeneration; swelling in the renal tubular epithelium; a narrowed lumen; interstitial angiectasis hyperemia, and a large number of infiltrated inflammatory cells, which were markedly aggravated by genipin pretreatment followed by LPS exposure.

3.4. UCP2 protects HK-2 cells against LPS-induced cytotoxicity

HK-2 cells were subjected to different concentrations of LPS (0, 1, 5, 10, 50, and 100 μg/ml) for 24 h, we found that when LPS concentration was up to 50 μg/ml, cell viability was remarkably decreased (Fig. 4A). These data indicated LPS damaged HK-2 cells in a dose-dependent manner, and the treatment of 100 μg/ml LPS for 24 h was selected as the condition for use in the subsequent experiments, except the experiment which is made to determine the release of inflammatory cytokines (100 μg/ml LPS for 6 h). As is shown in Fig. 4B and C, LPS exposure significantly inhibited cell viability and increased cell apoptosis. UCP2 overexpression alleviated the effects of LPS on cell viability and apoptosis, while UCP2 silencing aggravated these effects. In HK-2 cells transfected with LV5-UCP2 or si-UCP2, no significant effects on cell viability or cell apoptosis were observed compared the control group. Additionally, no significant differences in cell viability or cell apoptosis were found between control group, si-NC group, and LV5-NC group. We concluded that UCP2 played an important role in HK-2 cells under septic conditions and that UCP2 overexpression could protect HK-2 cells from LPS-induced cell injury and cell apoptosis.

3.5. UCP2 attenuates the LPS-induced inflammatory response

To investigate the effects abnormal UCP2 expression on the LPS-induced inflammatory response, the levels of multiple inflammatory cytokines, namely, TNF-α, IL-1β and IL-6, induced by LPS in vivo and in vitro were determined. As shown in Fig. 5A, we found that LPS effectively increased the mRNA levels of TNF-α, IL-1β and IL-6 in the kidney tissues of the LPS-induced mice compared with control group, and these levels were clearly increased further by pretreatment with genipin.

In addition, ELISAs and RT-qPCR analyses revealed that LPS-induced cells showed higher levels of inflammatory factors, including TNF-α, IL-1β and IL-6, than untreated cells (Fig. 5B and C). More importantly, UCP2 overexpression diminished the LPS-induced overproduction of these cytokines, and UCP2 silencing resulted in the opposite dynamic. Additionally, no significant effects on the levels of TNF-α, IL-1β or IL-6 were observed in HK-2 cells transfected with LV5-UCP2 or siRNA-UCP2 compared with control group. Furthermore, no significant differences in the levels of TNF-α, IL-1β or IL-6 were observed between control group, si-NC group, and LV5-NC group.

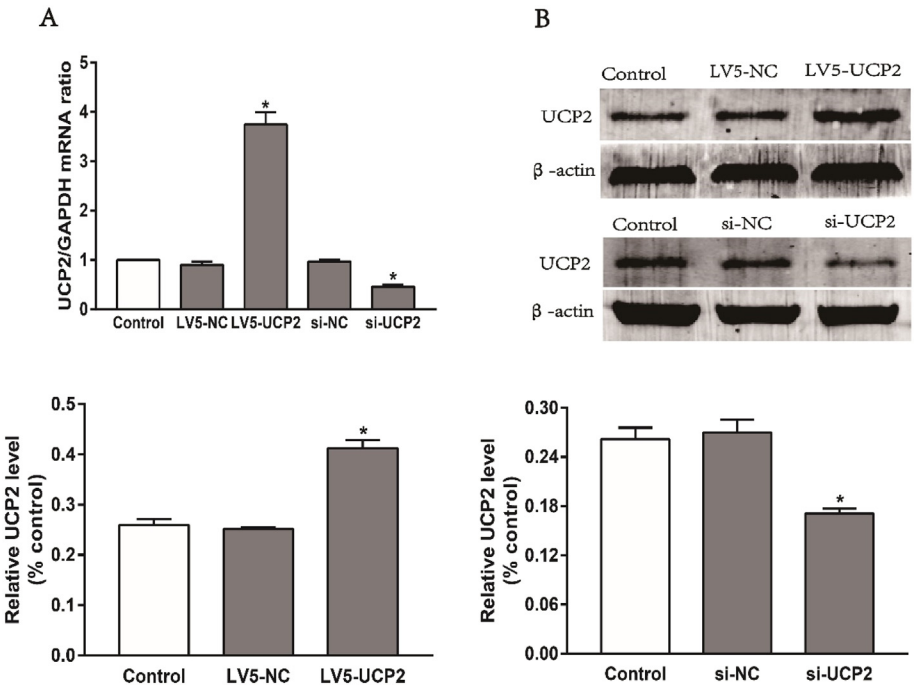

Fig. 1. Regulation of UCP2 expression by UCP2 recombinant lentiviral (LV5-UCP2) or si-UCP2 transfection in HK-2 cells. (A) UCP2 mRNA, (B) UCP2 protein expression in HK-2 cells transfected with LV5-UCP2 or si-UCP2 or control vectors. Data are expressed as the mean ± SD (n = 3–5 per group). *p < .05 versus control cells.

3.6. UCP2 inhibition by genipin pretreatment elicits the infiltration of macrophages into the kidneys of LPS-induced septic mice

To further investigate the infiltration of macrophages into kidney tissues, immunohistochemistry was used. As shown in Fig. 5D, the LPS challenge significantly promoted the infiltration of Galectin-3+ macrophages, and pretreatment with genipin resulted in more infiltration of Galectin-3+ macrophages.

3.7. UCP2 inhibits LPS-induced NF-κB activation in vivo and in vitro

NF-κB signaling pathway is a well-known target for the regulation of inflammatory response. LPS challenge contributed to the upregulation of phosphorylated IκBα and NF-κB p65. Fig. A and B showed that LPS challenge significantly elevated expressions of p-IκBα and p-p65, and pretreatment with genipin resulted in more expressions of p-IκBα and p-p65 compared with LPS-treated mice. Fig. 6C showed that compared with LV5-NC or si-NC group cells, respectively, the expressions of NF-κB signaling pathway related proteins, including p-IκBα and p-p65, were significantly up-regulated in LPS-treated cells. The LPS-induced cells with LV5-UCP2 showed obviously elevated expressions of p-IκBα and p-p65 compared with LV5-NC group, while the expressions of these proteins were significantly lower in LPS-induced cells with si-UCP2 than those in LPS-induced cells with si-NC. Neither LV5-UCP2 nor si-UCP2 transfection showed obvious effects on basal expressions of p-IκBα and p-p65 in HK-2 cells.

3.8. UCP2 restores mitochondrial membrane potential (MMP or ΔΨm) under septic conditions

The ΔΨm of the kidney tissue is shown in Fig. 7A. Confocal microscopy showed that ΔΨm was significantly decreased in LPS-induced mice compared with control mice, and that ΔΨm was further decreased in the mice pretreated with genipin.

The ΔΨm of the HK-2 cells was also assessed. FCM showed that ΔΨm was rapidly reduced in the LPS-treated cells compared with control cells, and the decrease in the ΔΨm of LPS-induced cells transfected with si-UCP2 were more significant than the decrease in the ΔΨm of LPS-induced cells (Fig. 7B and C). Confocal microscopy revealed the fluorescence changes in ΔΨm. The control group showed red fluorescence due to the high ΔΨm. Conversely, the treatment of HK-2 cells with LPS resulted in the dissipation of the ΔΨm, which manifested as increased green fluorescence. The green fluorescence intensity was markedly stronger in the LPS-induced cells with si-UCP2 than in the LPS-induced cells (Fig. 7D). si-UCP2 transfection showed no obvious effects on the basal ΔΨm of the HK-2 cells, and no significant differences in ΔΨm were observed between control group and si-NC group.

3.9. UCP2 attenuates the damage of mitochondrial ultrastructure under septic conditions

To characterize the changes in mitochondrial structure more objectively, the mitochondrial ultrastructure was examined by TEM. Fig. 8A shows that the mitochondrial ultrastructure was normal in control mice, while damage occurred in the LPS-induced mice. The damage to the mitochondrial ultrastructure was worse in the LPS + Genipin group than in LPS group.

TEM examination of HK-2 cells revealed that most of the mitochondrial membrane was intact, with a clear inner ridge, and was arranged more neatly under the control condition. However, after LPS exposure, the mitochondrial number decreased, and mitochondrial swelling and even vacuolization; the loss of matrix; and the disruption of crests were evident. Compared with control HK-2 cells, UCP2 overexpression alleviated the damage to mitochondrial ultrastructure induced by LPS exposure, but UCP2 knockdown cells showed further alterations in the aforementioned mitochondrial morphological and structural changes (Fig. 8B). In HK-2 cells transfected with LV5-UCP2 or si-UCP2, the mitochondrial ultrastructure showed no significant difference compared with control cells. Additionally, there were no significant differences in mitochondrial ultrastructure between control group, si-NC group, and LV5-NC group.

3.10. UCP2 inhibits ROS production, and increases the ATP levels and mtDNA content under septic conditions

To elucidate the role of UCP2 in mitochondrial function, intracellular ROS, ATP levels and mtDNA content were measured. DHE is

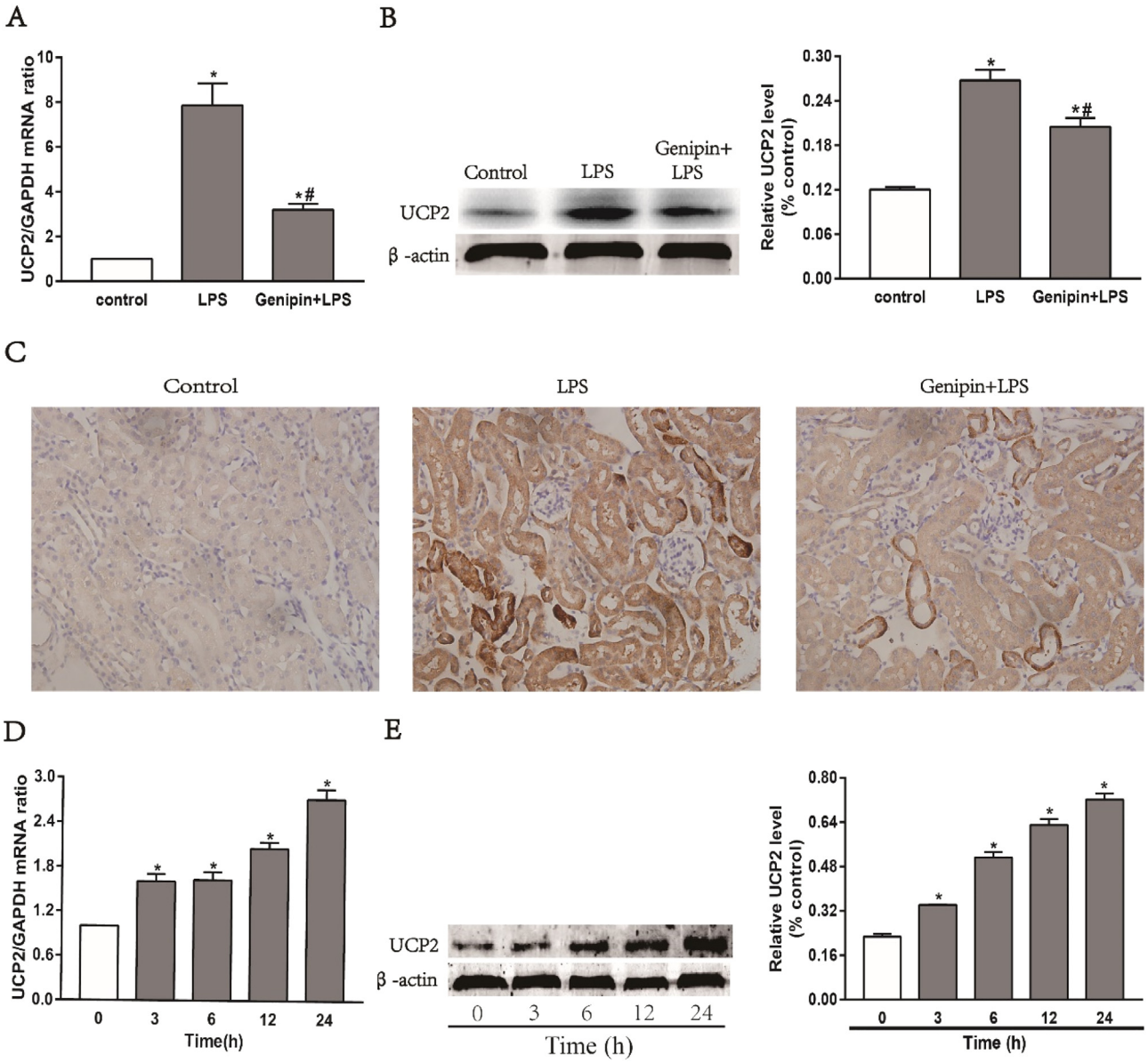

Fig. 2. Expression of UCP2 in mouse kidneys and in HK-2 cells under septic conditions. (A) UCP2 mRNA, (B) UCP2 protein expression in mouse kidneys. Data are expressed as the mean ± SD ($n = 8$ per group). *p < .05 versus control group, #p < .05 versus LPS group. (C) UCP2 protein expression was determined by immunohistochemical analysis (400× original magnification) in mice. (D) UCP2 mRNA, (E) UCP2 protein expression were determined in LPS-induced HK-2 cells. Data are expressed as the mean ± SD (n = 3–5 per group). *p < .05 versus control cells.

a fluorescent probe of ROS. Intracellular ROS production was quantified using FCM with DHE. FCM showed the upregulation of ROS production in LPS-induced HK-2 cells. UCP2 overexpression alleviated the abnormal ROS production induced by LPS exposure, but UCP2 silencing caused the abnormal ROS production to become more serious (Fig. 7E).

We next measured the ATP levels of the kidney tissues and found a significant decrease in the ATP levels of the LPS-treated mice compared with the control mice, and these levels were further decreased in the group that received genipin pretreatment (Fig. 7F). Moreover, Fig. 7G shows that compared with control group cells, the LPS group cells showed decreased ATP levels. Compared with LPS-treated cells, UCP2 overexpression in cells significantly increased ATP levels, and UCP2 knockdown further decreased the abnormal ATP levels induced by LPS.

mtDNA is also a sensitive indicator of mitochondrial function. The mtDNA content in the LPS mice was significantly lower than that in the control mice and was further decreased in the mice pretreated with genipin (Fig. 7H). At the same time, as shown in Fig. 7I, LPS induced a significant reduction in HK-2 cells. The mtDNA content of the LPS-induced cells with UCP2 overexpression was significantly higher than that of the LPS-induced cells and showed a sharp decline in the LPS-induced cells with UCP2 silencing compared with the LPS-induced cells. Neither LV5-UCP2 nor si-UCP2 transfection showed obvious effects on basal ROS production, the ATP level or the mtDNA content of HK-2 cells, and no significant differences in ROS production, the ATP level or mtDNA content were observed between control group, si-NC group, and LV5-NC group.

3.11. *UCP2 reduces oxidative stress under septic conditions*

As shown in Fig. 9A and C, LPS injection augmented oxidative stress in mouse kidneys. The malondialdehyde (MDA) levels and SOD activity were significantly increased and decreased, respectively, in LPS-treated mice compared with control mice. Genipin pretreatment significantly aggravated the increased oxidative stress by further increasing the MDA

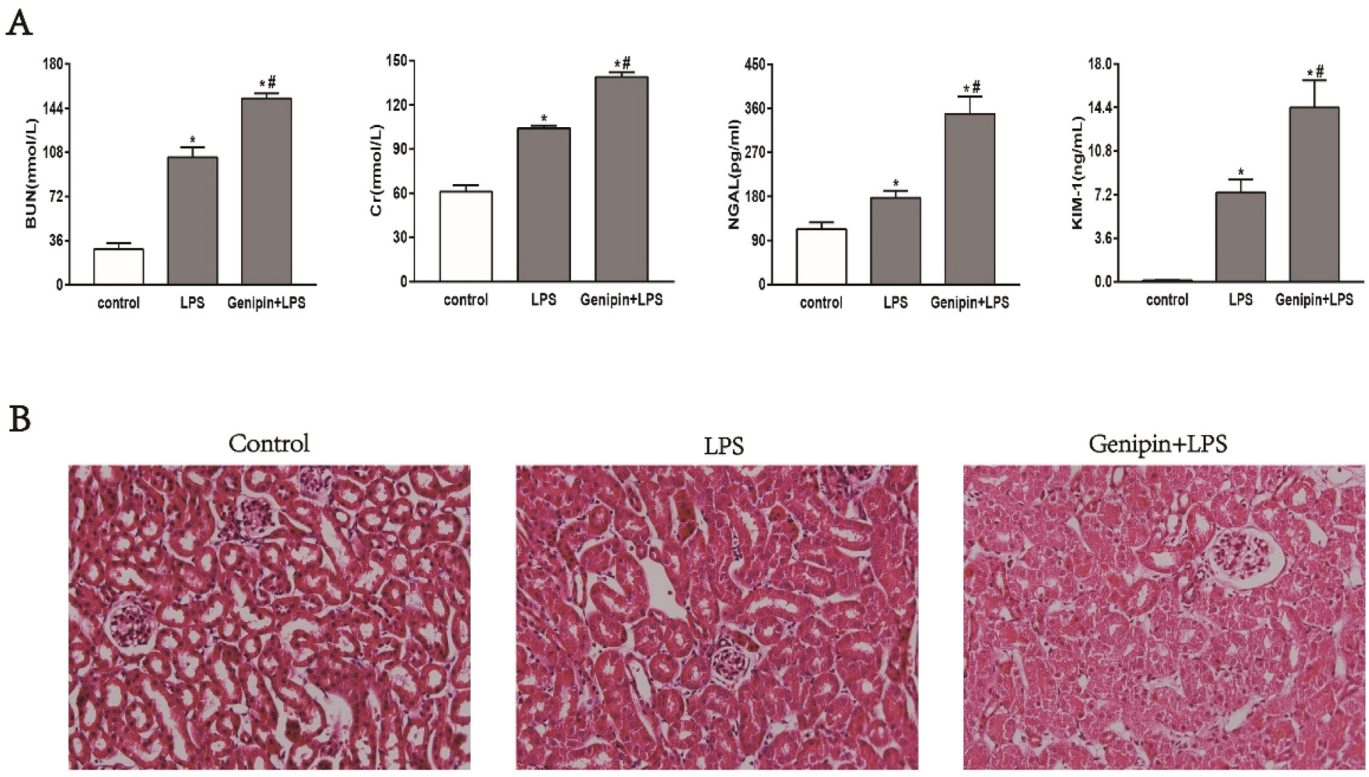

Fig. 3. UCP2 alleviates LPS-induced renal injury in vivo. (A) The serum BUN, Cr, KIM-1 and NGAL levels in mice. Data are expressed as the mean ± SD (n = 8 per group). *p < .05 versus the control mice, #p < .05 versus the LPS-treated mice. (B) H&E staining and histological observation of the kidneys (400× original magnification) in mice.

levels and decreasing SOD activity in mouse kidneys.

As shown in Fig. 9B and D, LPS enhanced the release of MDA and decreased SOD activity in HK-2 cells. UCP2 overexpression significantly decreased the MDA level and increased SOD activity against LPS-induced oxidative stress, while UCP2 silencing resulted in a further increase in the MDA level and a further decrease in SOD activity. Neither LV5-UCP2 nor si-UCP2 transfection showed obvious effects on the basal MDA level or SOD activity of HK-2 cells, and no significant differences were observed the control group, si-NC group, and LV5-NC group.

4. Discussion

In this manuscript, we address the principal findings as follows. First, UCP2 expression was upregulated in LPS-induced AKI, and LPS-induced upregulation of UCP2 expression was inhibited by pretreatment with genipin. Second, we further investigated the function of UCP2 using LV5-UCP2 or si-UCP2 to up- or down-regulate UCP2 expression under septic conditions. Third, LPS administration induced renal and HK-2 cell injury. UCP2 ameliorated the damage to renal function, reversed the histopathological changes, improved HK-2 cell viability and reduced cell apoptosis during sepsis. Furthermore, LPS treatment induced an inflammatory response, including inflammatory cytokine release, an elevation in inflammatory cell infiltration and NF-κB activation. UCP2 decreased the levels of inflammatory cytokines, attenuated inflammatory cell infiltration and inhibited NF-κB activation. Lastly, both the animal and cell models demonstrated that mitochondrial structure and function were disrupted, eventually leading to mitochondrial dysfunction. UCP2 ameliorated mitochondrial dysfunction, demonstrating that UCP2 may play a protective role in mitochondria in septic AKI. Additionally, UCP2 reduced oxidative stress under septic conditions. Together, these findings support the hypothesis that UCP2 plays an important and protective role in LPS-induced AKI.

Sepsis is not only a critical illness in the medical field worldwide but also an unsolved and disastrous problem for humans. LPS administration to experimental animals is frequently used as a surrogate model for human infectious sepsis [28]. In our study, treatment with LPS disrupted the structure and function of the kidney tissues, injured HK-2 cells and initiated the inflammatory response, demonstrating that our septic models had been generated successfully. These results are also in line with other experimental results [29,30]. Mitochondrial uncoupling proteins located in the mitochondrial inner membrane can promote proton leakage across the mitochondrial inner membrane [31]. UCP2 is the most well-known isoform in the UCP family and can be found in various tissues [32]. Its wide distribution is associated with a variety of functions, and UCP2 may protect organs under pathological conditions. Numerous studies have shown that UCP2 is involved in the regulation of inflammation, regulation of oxidative stress, maintenance of MMP and production of energy, which may be related to the pathophysiology of sepsis [33,34]. Previous reports have shown that UCP2 in blood cells might be a specific biomarker for sepsis and that the level of UCP2 is positively correlated with the severity of sepsis [35]. Recently, Chen et al. demonstrated that insulin ameliorated mitochondrial oxidative stress by upregulating UCP2 in septic AKI [25]. However, whether UCP2 plays an important role in septic AKI is still unclear. Our results showed that UCP2 expression was increased in septic AKI. To further determine the role of UCP2 in LPS-induced AKI, we transfected LV5-UCP2 or si-UCP2 into HK-2 cells to respectively overexpress or down-regulate UCP2 expression, and based on a previous study, we used genipin as a UCP2-specific inhibitor in vivo [23]. In vivo, treatment with LPS significantly increased the serum BUN, Cr, KIM-1 and NGAL levels, induced serious kidney pathological damage, elevated inflammatory cell infiltration, promoted inflammatory factor release and activated NF-κB. UCP2 inhibition with genipin increased the degree of LPS-induced renal injury and further promoted the inflammatory response. In vitro, LPS remarkably reduced cell viability, increased the cell apoptosis rate and promoted the inflammatory response. UCP2

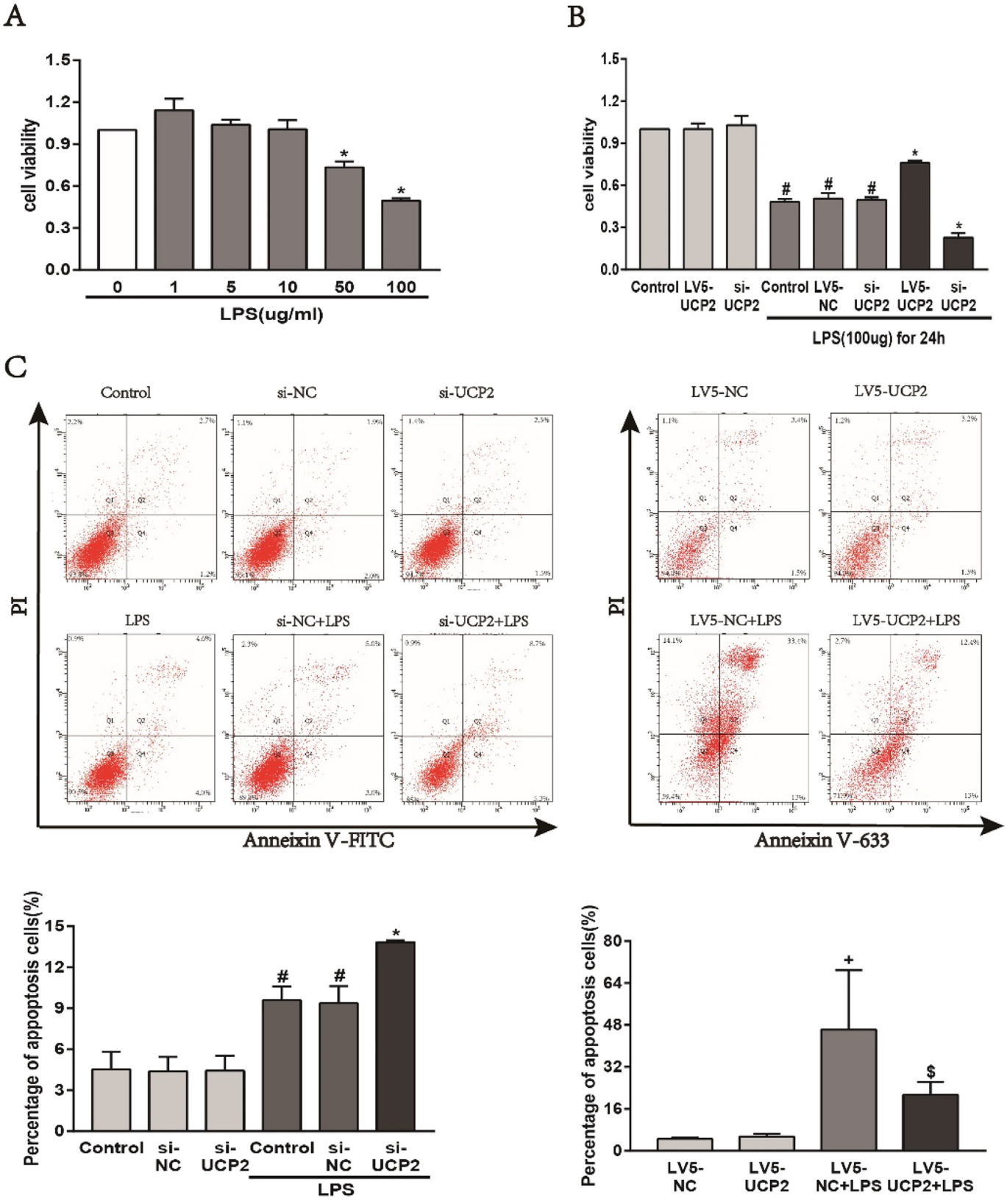

Fig. 4. UCP2 protects HK-2 cells against LPS-induced cytotoxicity and cell apoptosis. (A) Cell viability in different concentrations of LPS-induced HK-2 cells. Data are expressed as the mean ± SD (n = 3–5 per group). *p < .05 versus control cells. (B) Cell viability in LPS-induced HK-2 cells transfected with LV5-UCP2 or si-UCP2 or control vectors. (C) Cell apoptosis in LPS-induced HK-2 cells transfected with LV5-UCP2 or si-UCP2 or control vectors. Data are expressed as the mean ± SD (n = 3–5 per group). #p < .05 versus control cells, *p < .05 versus LPS group cells, +p < .05 versus LV5-NC group cells, $p < .05 versus LV5-NC + LPS group cells.

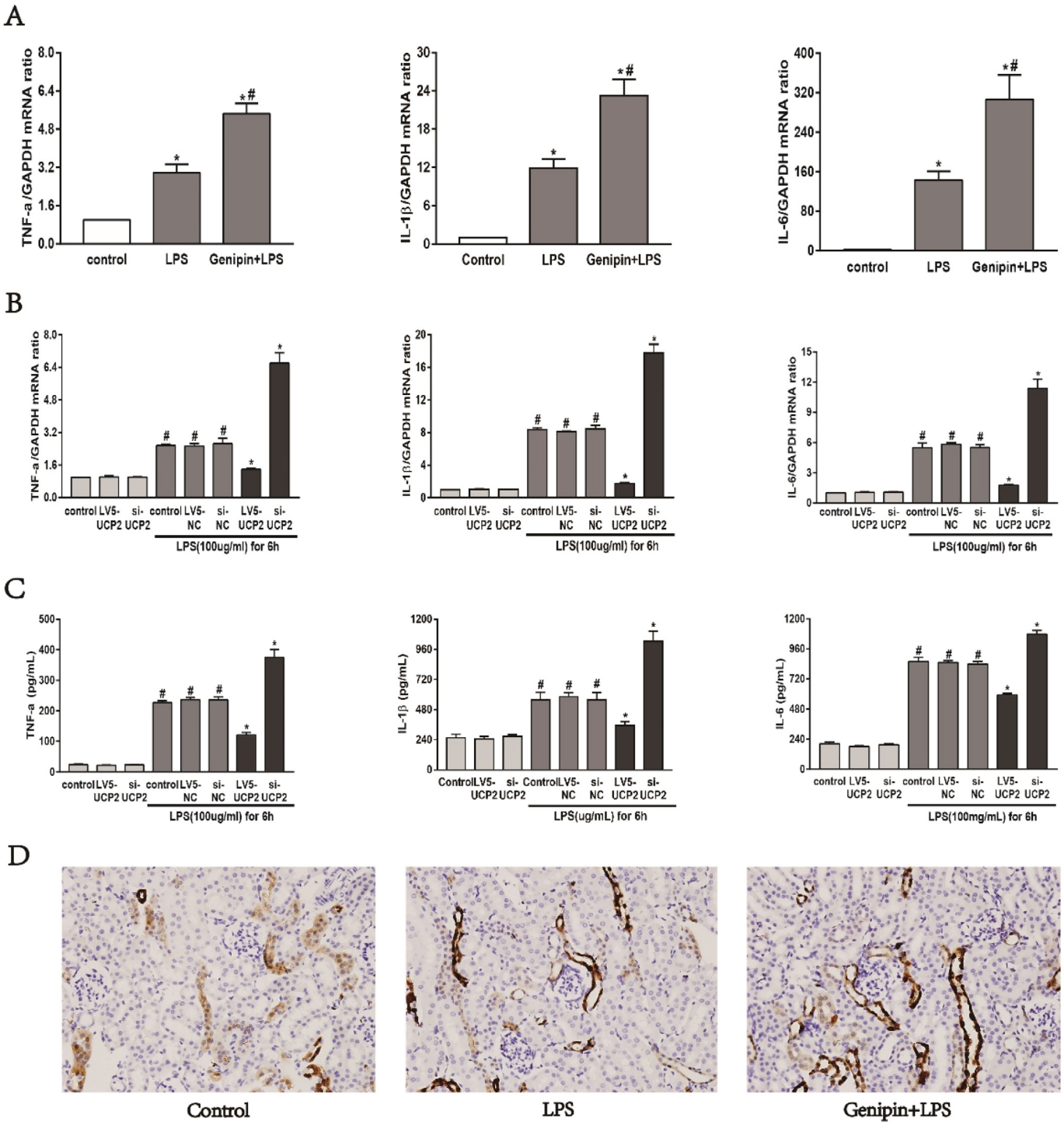

Fig. 5. UCP2 inhibits the production of cytokines by LPS in vitro and in vivo and reduces the infiltration of macrophages in kidneys of LPS-induced AKI mice. (A) The mRNA levels of TNF-α, IL-1β and IL-6 in mice. Data are expressed as the mean ± SD (n = 8 per group). *p < .05 versus control mice, #p < .05 versus LPS-treated mice. (B, C) The levels of TNF-α, IL-1β and IL-6 in LPS-induced HK-2 cells transfected with LV5-UCP2 or si-UCP2 or control vectors. Data are expressed as the mean ± SD (n = 3–5 per group). #p < .05 versus control cells, *p < .05 versus LPS group cells. (D) Infiltration of macrophages in kidneys of different group mice were determined by immunohistochemical analysis (400× original magnification).

overexpression significantly protected HK-2 cells from LPS-induced cell viability loss and cell apoptosis, while UCP2 knockdown resulted in increased cell loss and cell apoptosis compared with LPS treatment alone. Moreover, UCP2 overexpression significantly inhibited the release of inflammatory factors and NF-κB activation induced by LPS, and UCP2 knockdown further increased the release of inflammatory factors and promoted NF-κB activation in LPS-induced HK-2 cells. These observations suggested that UCP2 ameliorated the degree of LPS-induced AKI by inhibiting the inflammatory response and decreasing renal tubular epithelial cell apoptosis.

Mitochondria affect three key processes, namely, energy homeostasis, autophagy and the cell cycle that could potentially lead to apoptosis [36]. Therefore, mitochondrial dysfunction may play a prominent role in the development of organ dysfunction during sepsis.

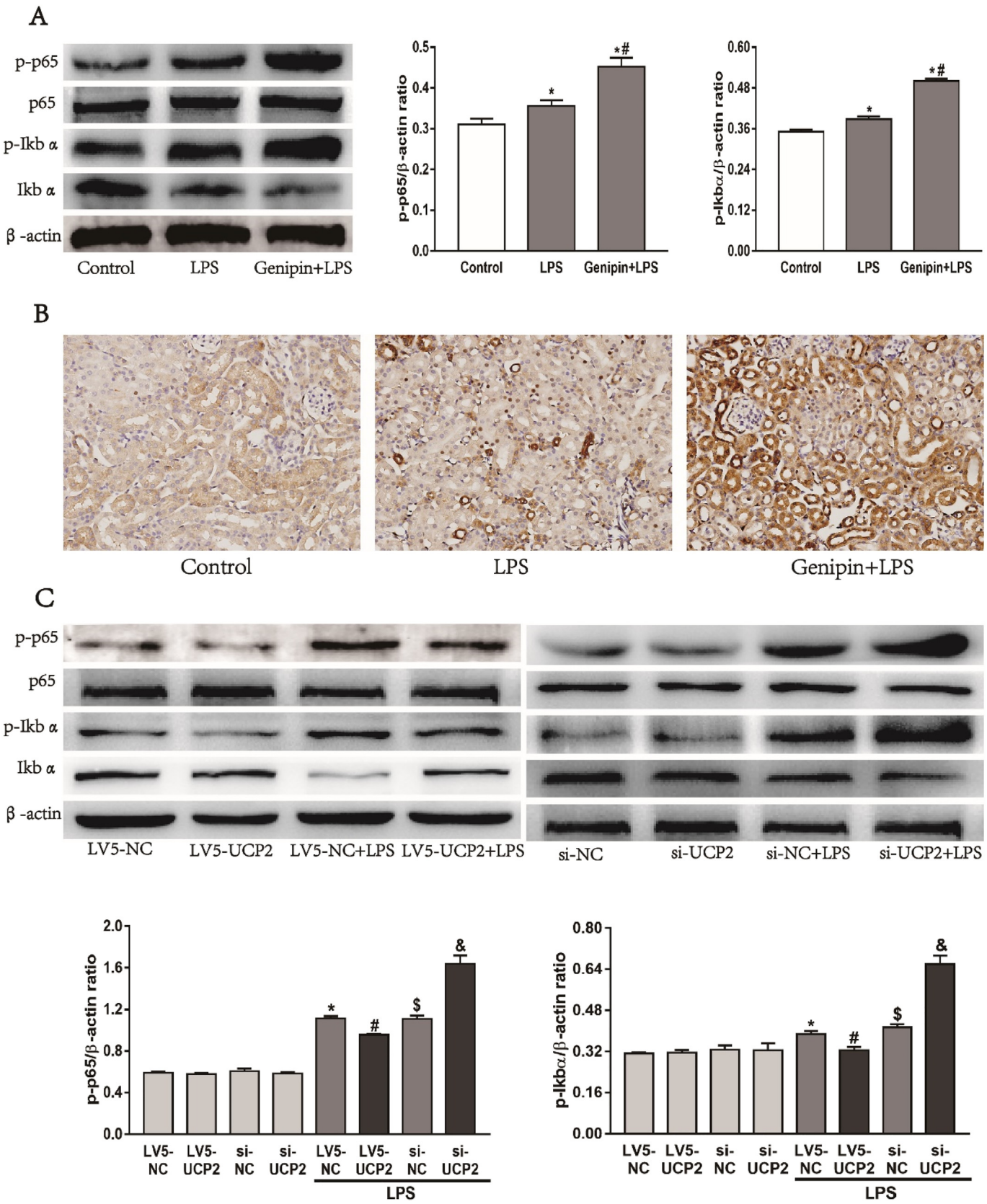

Fig. 6. UCP2 inhibits LPS-induced NF-κb activation in vivo and in vitro. (A, B) Western blot and immunohistochemical analysis (400× original magnification) showed UCP2 inhibits LPS-induced NF-κb activation in mice. Data are expressed as the mean ± SD (n = 8 per group). *p < .05 versus control mice, #p < .05 versus LPS-treated mice. (C) UCP2 inhibits LPS-induced NF-κb activation in HK-2 cells. Data are expressed as the mean ± SD (n = 3–5 per group). *p < .05 versus LV5-NC group cells, #p < .05 versus LV5-NC + LPS group cells, $p < .05 versus si-NC group cells, &p < .05 versus si-NC + LPS group cells.

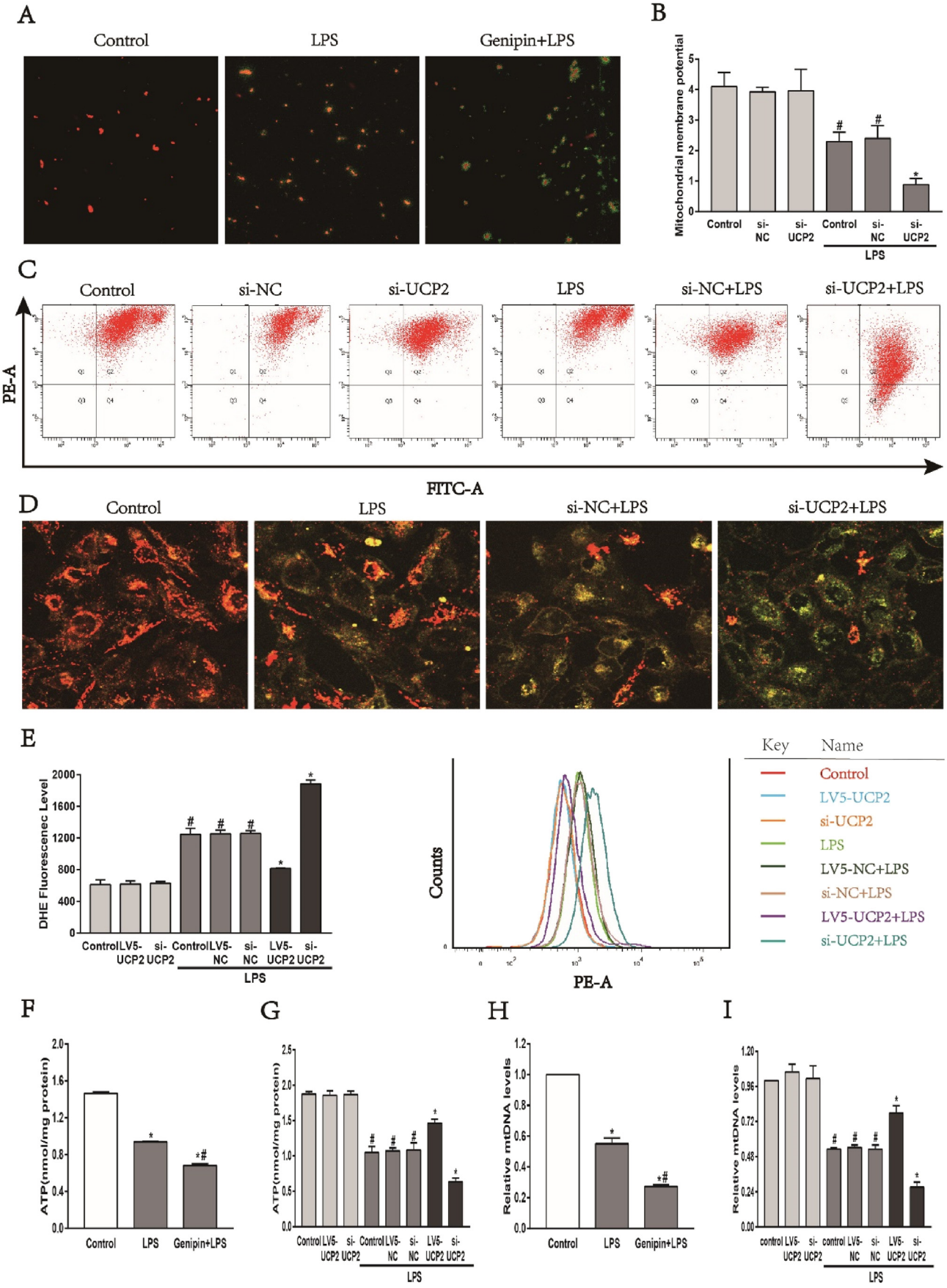

(caption on next page)

Fig. 7. Effects of UCP2 on mitochondrial function in vivo and in vitro. (A) The ΔΨm of the kidney tissue in different group mice were determined by confocal microscopy (400× original magnification). (B, C, D) Evaluation of ΔΨm in HK-2 cells transfected with si-UCP2 or si-NC by FCM and confocal microscopy. (E) Intracellular ROS levels in LPS-induced HK-2 cells transfected with LV5-UCP2 or si-UCP2 or control vectors. Data are expressed as the mean ± SD (n = 3-5per group). $^{\#}p < .05$ versus control cells, $^{*}p < .05$ versus LPS group cells. (F, G) The ATP levels of the kidney tissues and HK-2 cells. (H, I) Relative mtDNA copy numbers of the kidney tissues and HK-2 cells. Data are expressed as the mean ± SD (n = 3 per group). $^{\#}p < .05$ versus LPS-treated mice (F, H) and control cells (G, I), $^{*}p < .05$ versus control mice (F, H) and the LPS-treated cells (G, I).

UCP2 localizes to mitochondria and plays an important role in maintaining normal mitochondrial structure and function. We previously observed that the silencing of UCP2 by small interfering RNA aggravated mitochondrial dysfunction in cardiomyocytes under septic conditions [37]. In our study, TEM showed that the mitochondrial ultrastructure was damaged after LPS exposure, and this damage was worse in the LPS + genipin group. In vitro, UCP2 overexpression attenuated this adverse effect in LPS-induced HK-2 cells, while UCP2 knockdown showed the opposite dynamic.

MMP reflects the performance of the mitochondrial electron transport chain (ETC), which is often used as an indicator of the pathological disorder of the mitochondrion. The intrinsic target of UCP2 is the H+ channel that is located on the inner mitochondrial membrane, and UCP2 promotes proton leakage, which can influence MMP [19]. The outcome of uncoupling is the collapse of MMP, which is caused by proton leakage from the intermembrane space into the matrix [38]. In the present study, treatment with LPS induced the disruption of MMP, which was further decreased by pretreatment with genipin in mice. In vitro, UCP2 knockdown resulted in further disruption of MMP, which was consistent with the results of a previous study that used a model of sepsis [19]. These observations confirmed that UCP2 could restore the disruption of MMP induced by the LPS challenge in HK-2 cells and

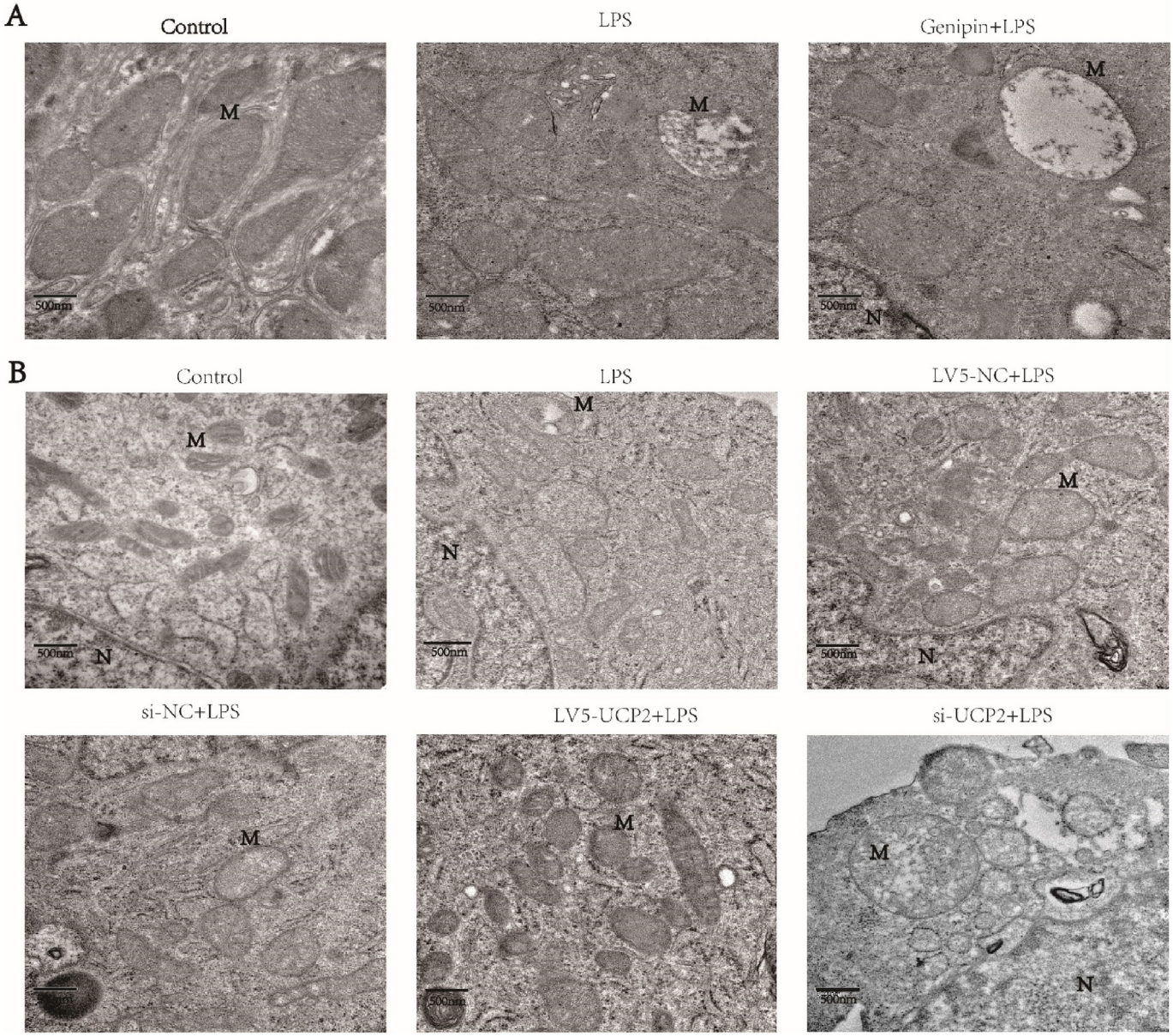

Fig. 8. Effects of UCP2 on mitochondrial ultrastructure in vivo and in vitro under septic conditions. (A, B) Mitochondrial ultrastructure of the kidney tissues and HK-2 cells were scanned using a transmission electron microscope (40,000× original magnification). M for mitochondrion, N for nucleus.

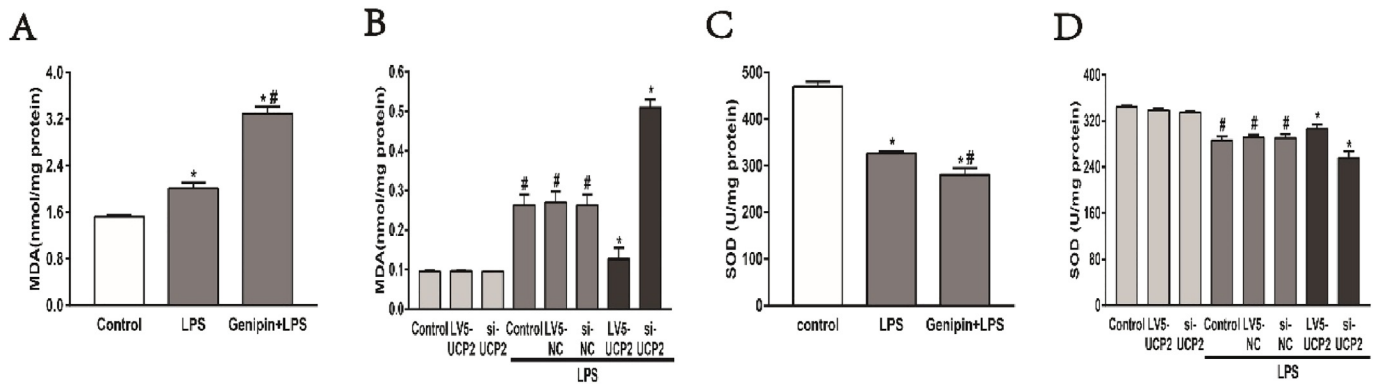

Fig. 9. UCP2 ameliorates oxidative stress in vivo and in vitro under septic conditions. (A, B) MDA levels of mouse kidneys and HK-2 cells. (C, D) SOD activity of mouse kidney tissues and HK-2 cells. Data are expressed as the mean ± SD (n = 6 per group). #p < .05 versus LPS-treated mice (A, C) and control cells (B, D), *p < .05 versus control mice (A, C) and LPS-treated cells (B, D).

mice.

Several studies have reported that ROS play a crucial role in the physiological process of sepsis [39]. During LPS-induced shock, the excessive release of ROS may trigger hyperactivation of innate immune cells, the overexpression of cytokines, and even end-stage organ injury [40]. Mitochondria are the main source and target of ROS within cells. In a previous study, Quoilin [41] et al. noted that the mechanism of ROS-induced ROS formation might be a main cause of mitochondrial dysfunction. The authors revealed that after being targeted by oxidants, mitochondria became a producer of ROS, thus contributing to aggravating mitochondrial dysfunction. An previous study suggested that UCP2 is a negative regulator of ROS production that functions via by reducing MMP [22]. In the present study, the LPS challenge caused an apparent increase in intracellular ROS production, and in vitro transfection of HK-2 cells with LV5-UCP2 reduced LPS-induced intracellular ROS overproduction. As expected, UCP2 knockdown enhanced LPS-induced the superoxide component of intracellular ROS production in HK-2 cells. Our results are in line with some in vivo and in vitro studies showing that UCP2 carries out protective functions against oxidative stress under septic or other conditions by suppressing ROS generation, NADPH oxidase production, iNOS expression and NO production [37,42–45].

ROS can oxidatively impair mtDNA [46]. In addition, mtDNA is positively correlated with the expression of multiple proteins associated with mitochondrial biogenesis, such as PGC-1a, NRF1, NRF2, and TFAM [47]. In the current study, treatment with LPS resulted in damage to mtDNA, which was further enhanced by pretreatment with genipin in mice. In vitro, UCP2 overexpression reversed the damage to mtDNA induced by LPS, and UCP2 knockdown further reduced the mtDNA content. Furthermore, cellular ATP is another indicator of mitochondrial function. Mitochondria are the main source of ATP, which is the only universal energy-yielding currency in cells. ATP synthesis relies on the coupling of electron transport through the ETC to the proton motive force. The coupling procedure is regulated by proton leakage through the mitochondrial inner membrane, which is partly mediated by UCP2. However, the association between UCP2 and ATP remains controversial. Some studies have demonstrated that UCP2 activity may lead to decreased ATP levels [12,37,48], while others have suggested that overexpression of UCP2 can elevate ATP levels [22,23,49]. In this study, sepsis led to a low level of ATP, which was further reduced by genipin pretreatment. In vitro, UCP2 overexpression obviously increased ATP levels after the LPS challenge, while UCP2 knockdown showed an accelerated decrease in ATP levels. The ATP level was increased by UCP2 in septic AKI, possibly because of the restored mitochondrial ultrastructure and the elevated mtDNA content. From our results, we inferred that UCP2 could alleviate mitochondrial function in LPS-induced AKI by blocking the dissipation of MMP, thereby inhibiting intracellular ROS production and increasing the cellular ATP levels and mtDNA content.

The development of organ dysfunction under septic conditions is now regarded as resulting from oxidative damage to mitochondria. The main cause of oxidative stress is the presence of ROS, which serve as a marker of the oxidative stress level. Many studies have demonstrated that UCP2 can reduce oxidative stress in sepsis or other models [25,43,50–52]. In the present study, we found that in the LPS group, the marker of oxidative stress (MDA) was suppressed and that antioxidants (SOD activity) were enhanced. In vivo, pretreatment with genipin accelerated this effect. In vitro, this effect was inhibited by UCP2 overexpression and accelerated by UCP2 downregulation. Based on the observations of the present study, we propose that UCP2 reduces the level of oxidative stress in LPS-induced AKI.

In conclusion, our present study provides evidence that UCP2 is expressed in kidney tissue and that UCP2 levels increase in response to LPS exposure. UCP2 may protect against LPS-induced AKI via ameliorating the damage of mitochondrial morphology and function, anti-inflammation and antioxidant activities. Our results suggest that mitochondria may be the main target for UCP2-mediated nephroprotection, which indicates that targeting upregulated UCP2 levels in mitochondria will be a new therapeutic approach for septic AKI.

Acknowledgments

The current study was supported by the National Natural Science Foundation of China (grant no. 81272070).

Conflicts of interest

None.

References

[1] M. Singer, C.S. Deutschman, C.W. Seymour, M. Shankar-Hari, D. Annane, M. Bauer, et al., The third international consensus definitions for sepsis and septic shock (sepsis-3), Jama 315 (2016) 801–810.
[2] D. De Backer, T. Dorman, Surviving sepsis guidelines: a continuous move toward better care of patients with Sepsis, Jama 317 (2017) 807–808.
[3] C.W. Seymour, V.X. Liu, T.J. Iwashyna, F.M. Brunkhorst, T.D. Rea, A. Scherag, et al., Assessment of clinical criteria for Sepsis: for the third international consensus definitions for sepsis and septic shock (sepsis-3), Jama 315 (2016) 762–774.
[4] E.K. Stevenson, A.R. Rubenstein, G.T. Radin, R.S. Wiener, A.J. Walkey, Two decades of mortality trends among patients with severe sepsis: a comparative meta-analysis*, Crit. Care Med. 42 (2014) 625–631.
[5] D.F. Gaieski, J.M. Edwards, M.J. Kallan, B.G. Carr, Benchmarking the incidence and mortality of severe sepsis in the United States, Crit. Care Med. 41 (2013) 1167–1174.
[6] D.C. Angus, T. van der Poll, Severe sepsis and septic shock, N. Engl. J. Med. 369 (2013) 840–851.
[7] N.K. Adhikari, R.A. Fowler, S. Bhagwanjee, G.D. Rubenfeld, Critical care and the

global burden of critical illness in adults, Lancet 376 (2010) 1339–1346.
[8] J. Zhang, G. Ankawi, J. Sun, K. Digvijay, Y. Yin, M.H. Rosner, et al., Gut-kidney crosstalk in septic acute kidney injury, Crit. Care 22 (2018) 117.
[9] Mason A.J. AC, N. Thirunavukkarasu, G.D. Perkins, M. Cecconi, M. Cepkova, et al., Effect of early vasopressin vs norepinephrine on kidney failure in patients with septic shock: the VANISH randomized clinical trial, Jama 316 (2016) 509–518, https://doi.org/10.1001/jama.2017.0059Gordon.
[10] P. Pickkers, R.L. Mehta, P.T. Murray, M. Joannidis, B.A. Molitoris, J.A. Kellum, et al., Effect of human recombinant alkaline phosphatase on 7-day creatinine clearance in patients with sepsis-associated acute kidney injury: a randomized clinical trial, Jama 320 (2018) 1998–2009.
[11] H. Gomez, J.A. Kellum, Sepsis-induced acute kidney injury, Curr. Opin. Crit. Care 22 (2016) 546–553.
[12] H. Zhang, Y.W. Feng, Y.M. Yao, Potential therapy strategy: targeting mitochondrial dysfunction in sepsis, Mil. Med. Res. 5 (2018) 41.
[13] H.F. Galley, Bench-to-bedside review: targeting antioxidants to mitochondria in sepsis, Crit. Care 14 (2010) 230.
[14] S.M. Parikh, Y. Yang, L. He, C. Tang, M. Zhan, Z. Dong, Mitochondrial function and disturbances in the septic kidney, Semin. Nephrol. 35 (2015) 108–119.
[15] A.D. Cherry, C.A. Piantadosi, Regulation of mitochondrial biogenesis and its intersection with inflammatory responses, Antioxid. Redox Signal. 22 (2015) 965–976.
[16] A. Linkermann, G. Chen, G. Dong, U. Kunzendorf, S. Krautwald, Z. Dong, Regulated cell death in AKI, J. Am. Soc. Nephrol. 25 (2014) 2689–2701.
[17] X.X. Yu, J.L. Barger, B.B. Boyer, M.D. Brand, G. Pan, S.H. Adams, Impact of endotoxin on UCP homolog mRNA abundance, thermoregulation, and mitochondrial proton leak kinetics, Am. J. Physiol. Endocrinol. Metab. 279 (2000) E433–E446.
[18] D. Ricquier, B. Miroux, A.M. Cassard-Doulcier, C. Levi-Meyrueis, C. Gelly, S. Raimbault, et al., Contribution to the identification and analysis of the mitochondrial uncoupling proteins, J. Bioenerg. Biomembr. 31 (1999) 407–418.
[19] P. Pan, H. Zhang, L. Su, X. Wang, D. Liu, Melatonin balance the autophagy and apoptosis by regulating UCP2 in the LPS-induced cardiomyopathy, Molecules 23 (2018).
[20] W. Chen, S. Luo, P. Xie, T. Hou, T. Yu, X. Fu, Overexpressed UCP2 regulates mitochondrial flashes and reverses lipopolysaccharide-induced cardiomyocytes injury, Am. J. Transl. Res. 10 (2018) 1347–1356.
[21] M. Jaburek, J. Jezek, P. Jezek, Cytoprotective activity of mitochondrial uncoupling protein-2 in lung and spleen, FEBS Open Bio 8 (2018) 692–701.
[22] Y. Shang, Y. Liu, L. Du, Y. Wang, X. Cheng, W. Xiao, et al., Targeted expression of uncoupling protein 2 to mouse liver increases the susceptibility to lipopolysaccharide/galactosamine-induced acute liver injury, Hepatology 50 (2009) 1204–1216.
[23] Q. Wang, J. Wang, M. Hu, Y. Yang, L. Guo, J. Xu, et al., Uncoupling protein 2 increases susceptibility to lipopolysaccharide-induced acute lung injury in mice, Mediat. Inflamm. 2016 (2016) 9154230.
[24] K. Le Minh, A. Kuhla, K. Abshagen, T. Minor, J. Stegemann, S. Ibrahim, et al., Uncoupling protein-2 deficiency provides protection in a murine model of endotoxemic acute liver failure, Crit. Care Med. 37 (2009) 215–222.
[25] G.D. Chen, J.L. Zhang, Y.T. Chen, J.X. Zhang, T. Wang, Q.Y. Zeng, Insulin alleviates mitochondrial oxidative stress involving upregulation of superoxide dismutase 2 and uncoupling protein 2 in septic acute kidney injury, Exp. Ther. Med. 15 (2018) 3967–3975.
[26] R.A. Zager, A.C. Johnson, S.Y. Hanson, S. Lund, Acute nephrotoxic and obstructive injury primes the kidney to endotoxin-driven cytokine/chemokine production, Kidney Int. 69 (2006) 1181–1188.
[27] R. Araki, Y. Hiraki, T. Yabe, Genipin attenuates lipopolysaccharide-induced persistent changes of emotional behaviors and neural activation in the hypothalamic paraventricular nucleus and the central amygdala nucleus, Eur. J. Pharmacol. 741 (2014) 1–7.
[28] S. Goncalves, R. Fernandez-Sanchez, M.D. Sanchez-Nino, A. Tejedor, F. Neria, J. Egido, et al., Tyrphostins as potential therapeutic agents for acute kidney injury, Curr. Med. Chem. 17 (2010) 974–986.
[29] W. Huang, X. Lan, X. Li, D. Wang, Y. Sun, Q. Wang, et al., Long non-coding RNA PVT1 promote LPS-induced septic acute kidney injury by regulating TNFalpha and JNK/NF-kappaB pathways in HK-2 cells, Int. Immunopharmacol. 47 (2017) 134–140.
[30] S. Zhang, J. Ma, L. Sheng, D. Zhang, X. Chen, J. Yang, et al., Total coumarins from hydrangea paniculata show renal protective effects in lipopolysaccharide-induced acute kidney injury via anti-inflammatory and antioxidant activities, Front. Pharmacol. 8 (2017) 872.
[31] M.T. Oliveira, R. Garesse, L.S. Kaguni, Animal models of mitochondrial DNA transactions in disease and ageing, Exp. Gerontol. 45 (2010) 489–502.
[32] M. Donadelli, I. Dando, C. Fiorini, M. Palmieri, UCP2, a mitochondrial protein regulated at multiple levels, Cell. Mol. Life Sci. 71 (2014) 1171–1190.
[33] F.L. Sheeran, S. Pepe, Energy deficiency in the failing heart: linking increased reactive oxygen species and disruption of oxidative phosphorylation rate, Biochim. Biophys. Acta 1757 (2006) 543–552.
[34] M. Singer, The role of mitochondrial dysfunction in sepsis-induced multi-organ failure, Virulence 5 (2014) 66–72.
[35] Z.M. Jiang, Q.H. Yang, C.Q. Zhu, UCP2 in early diagnosis and prognosis of sepsis, Eur. Rev. Med. Pharmacol. Sci. 21 (2017) 549–553.
[36] H. Gomez, C. Ince, D. De Backer, P. Pickkers, D. Payen, J. Hotchkiss, et al., A unified theory of sepsis-induced acute kidney injury: inflammation, microcirculatory dysfunction, bioenergetics, and the tubular cell adaptation to injury, Shock 41 (2014) 3–11.
[37] G. Zheng, J. Lyu, S. Liu, J. Huang, C. Liu, D. Xiang, et al., Silencing of uncoupling protein 2 by small interfering RNA aggravates mitochondrial dysfunction in cardiomyocytes under septic conditions, Int. J. Mol. Med. 35 (2015) 1525–1536.
[38] J.S. Moon, S. Lee, M.A. Park, I.I. Siempos, M. Haslip, P.J. Lee, et al., UCP2-induced fatty acid synthase promotes NLRP3 inflammasome activation during sepsis, J. Clin. Invest. 125 (2015) 665–680.
[39] K.H. Krause, K. Bedard, NOX enzymes in immuno-inflammatory pathologies, Semin. Immunopathol. 30 (2008) 193–194.
[40] X. Kong, R. Thimmulappa, P. Kombairaju, S. Biswal, NADPH oxidase-dependent reactive oxygen species mediate amplified TLR4 signaling and sepsis-induced mortality in Nrf2-deficient mice, J. Immunol. 185 (2010) 569–577.
[41] C. Quoilin, A. Mouithys-Mickalad, S. Lecart, M.P. Fontaine-Aupart, M. Hoebeke, Evidence of oxidative stress and mitochondrial respiratory chain dysfunction in an in vitro model of sepsis-induced kidney injury, Biochim. Biophys. Acta 1837 (2014) 1790–1800.
[42] T. Kizaki, K. Suzuki, Y. Hitomi, N. Taniguchi, D. Saitoh, K. Watanabe, et al., Uncoupling protein 2 plays an important role in nitric oxide production of lipopolysaccharide-stimulated macrophages, Proc. Natl. Acad. Sci. U. S. A. 99 (2002) 9392–9397.
[43] T. Cao, Y. Dong, R. Tang, J. Chen, C.Y. Zhang, K. Zen, Mitochondrial uncoupling protein 2 protects splenocytes from oxidative stress-induced apoptosis during pathogen activation, Cell. Immunol. 286 (2013) 39–44.
[44] R. De Simone, M.A. Ajmone-Cat, M. Pandolfi, A. Bernardo, C. De Nuccio, L. Minghetti, et al., The mitochondrial uncoupling protein-2 is a master regulator of both M1 and M2 microglial responses, J. Neurochem. 135 (2015) 147–156.
[45] M. Toral, M. Romero, R. Jimenez, I. Robles-Vera, J. Tamargo, M.C. Martinez, et al., Role of UCP2 in the protective effects of PPARbeta/delta activation on lipopolysaccharide-induced endothelial dysfunction, Biochem. Pharmacol. 110-111 (2016) 25–36.
[46] I. Larosche, P. Letteron, A. Berson, B. Fromenty, T.T. Huang, R. Moreau, et al., Hepatic mitochondrial DNA depletion after an alcohol binge in mice: probable role of peroxynitrite and modulation by manganese superoxide dismutase, J. Pharmacol. Exp. Ther. 332 (2010) 886–897.
[47] R. Zamora-Mendoza, H. Rosas-Vargas, M.T. Ramos-Cervantes, P. Garcia-Zuniga, H. Perez-Lorenzana, P. Mendoza-Lorenzo, et al., Dysregulation of mitochondrial function and biogenesis modulators in adipose tissue of obese children, Int. J. Obes. 42 (2018) 618–624.
[48] M. Haslip, I. Dostanic, Y. Huang, Y. Zhang, K.S. Russell, M.J. Jurczak, et al., Endothelial uncoupling protein 2 regulates mitophagy and pulmonary hypertension during intermittent hypoxia, Arterioscler. Thromb. Vasc. Biol. 35 (2015) 1166–1178.
[49] P. Eyenga, D. Roussel, J. Morel, B. Rey, C. Romestaing, V. Gueguen-Chaignon, et al., Time course of liver mitochondrial function and intrinsic changes in oxidative phosphorylation in a rat model of sepsis, Intensive Care Med. Exp. 6 (2018) 31.
[50] Y. Teshima, M. Akao, S.P. Jones, E. Marban, Uncoupling protein-2 overexpression inhibits mitochondrial death pathway in cardiomyocytes, Circ. Res. 93 (2003) 192–200.
[51] S.E. Tang, C.P. Wu, S.Y. Wu, C.K. Peng, W.C. Perng, B.H. Kang, et al., Stanniocalcin-1 ameliorates lipopolysaccharide-induced pulmonary oxidative stress, inflammation, and apoptosis in mice, Free Radic. Biol. Med. 71 (2014) 321–331.
[52] K.A. Steen, H. Xu, D.A. Bernlohr, FABP4/aP2 regulates macrophage redox signaling and Inflammasome activation via control of UCP2, Mol. Cell. Biol. 37 (2017).